AIP | Journal of Applied Physics

Recalescence after bulk solidification in germanium films melted by ns laser pulses

J. Armengol, F. Vega, N. Chaoui, J. Solis, and C. N. Afonso

Citation: J. Appl. Phys. 93, 1505 (2003); doi: 10.1063/1.1534374
View online: http://dx.doi.org/10.1063/1.1534374
View Table of Contents: http://jap.aip.org/resource/1/JAPIAU/v93/i3
Published by the American Institute of Physics.

Related Articles

Thermoelectric magnetic force acting on the solid during directional solidification under a static magnetic field
Appl. Phys. Lett. 101, 251904 (2012)

Structural features and high quasi-static strain rate sensitivity of Au49Cu26.9Ag5.5Pd2.3Si16.3 bulk metallic glass
Appl. Phys. Lett. 101, 241905 (2012)

First principle molecular dynamic simulation of the rapid solidification process of Ca50Mg20Cu30 alloy
J. Appl. Phys. 112, 073517 (2012)

Effect of tungsten metal particle sizes on the solubility of molten alloy melt: Experimental observation of Gibbs-Thomson effect in nanocomposites
Appl. Phys. Lett. 101, 124103 (2012)

Nanosize icosahedral quasicrystal in Mg90Ca10 glass: An ab initio molecular dynamics study
J. Chem. Phys. 137, 034503 (2012)

Additional information on J. Appl. Phys.

Journal Homepage: http://jap.aip.org/
Journal Information: http://jap.aip.org/about/about_the_journal
Top downloads: http://jap.aip.org/features/most_downloaded
Information for Authors: http://jap.aip.org/authors

ADVERTISEMENT

Downloaded 23 Jan 2013 to 161.111.22.141. Redistribution subject to AIP license or copyright; see http://jap.aip.org/about/rights_and_permissions

Recalescence *after* bulk solidification in germanium films melted by ns laser pulses

J. Armengol and F. Vega[a)]
Departament d'Optica i Optometria, Universitat Politècnica de Catalunya, C/Violinista Vellsolà 37 08222-Terrassa, Spain

N. Chaoui,[b)] J. Solis, and C. N. Afonso
Instituto de Óptica del Consejo Superior de Investigaciones Científicas, C/Serrano 121 28006-Madrid, Spain

(Received 5 August 2002; accepted 7 November 2002)

Rapid solidification dynamics in amorphous germanium films melted by nanosecond laser pulses has been analyzed by means of single-shot subnanosecond time resolved reflectivity measurements using a streak camera based setup. The results show that once a minimum melt depth is induced, a bulk solidification process followed by the release of the solidification enthalpy dominates the solidification scenario. Moreover, the laser-melted material *solidifies completely* before being remelted as a consequence of the solidification enthalpy release, something only observed, up to date, upon irradiation with picosecond laser pulses. © *2003 American Institute of Physics.*
[DOI: 10.1063/1.1534374]

I. INTRODUCTION

The possibility of using pulsed laser irradiation to crystallize amorphous Si (*a*-Si) films on low cost substrates in order to produce thin film transistors[1] for flat panel displays and high efficiency solar cells[2] has renewed the interest in pulsed laser induced melting and rapid solidification phenomena in semiconductors.[3–6] In materials like Si and Ge, the lower melting point of the amorphous phase with respect to the crystalline one makes it possible to produce a highly supercooled liquid by the rapid melting of an amorphous film with a short laser pulse. Depending on the characteristics of heat flow to the substrate, the supercooled liquid can resolidify in the crystalline or amorphous phases or in a mixture of both through different solidification scenarios. In particular, it has been shown that bulk, interfacial, and surface-initiated solidification can be selectively induced or prevented by a careful selection of the parameters that determine the heat flow to the substrate like laser pulse fluence, film thickness, and type of substrate.[7,8] From the point of view of commercial applications of pulsed laser melting for crystallization of thin films, these findings are of great importance to control the phase to be obtained.

In the case of bulk solidification, the formation of a highly supercooled molten pool with a negligible in-depth thermal gradient promotes the nucleation of the solid phase throughout the whole molten volume at extremely high nucleation rates.[9–12] This leads to a massive release of the solidification enthalpy. As a consequence, the material gets reheated after the initial solidification stage in a process usually referred to as *recalescence* and can eventually remelt. The final state of the material (i.e., the fraction of amorphous to crystalline phases upon solidification) obeys to a complex balance given by the initial supercooling and nucleation rate, the initial fraction of amorphous and crystalline material nucleated, the amount of solidification enthalpy released, and the heat flow to the substrate.

It has been recently shown that upon picosecond laser pulse irradiation, the remelting process induced by recalescence can occur after the material has completely solidified in the initial stage.[7,13] This result was very much in contrast with the interpretation given to earlier reported results upon nanosecond pulse irradiation of Ge and Si semiconductors[9–11] in which recalescence effects were thought to be responsible for a slowdown of the solidification process.

Since nanosecond pulses are used in almost all commercial applications, it is of great interest to analyze in detail the rapid solidification dynamics of amorphous-Ge films irradiated with ns laser pulses and to compare the results to those obtained upon picosecond pulses. We have used real time reflectivity measurements with subnanosecond resolution. The film thickness and pulse fluence have been the parameters used to modify the heat flow rate from the melted layer to the substrate and thus to access *to* the different solidification scenarios. The experiments were carried out in conditions similar to those of Ref. 7 but using nanosecond instead of picosecond pulses. The results obtained provide unambiguous evidence for the occurrence of complete solidification before recalescence-induced remelting as a consequence of the release of the solidification enthalpy.

II. EXPERIMENTS AND SIMULATION

The samples used were amorphous Ge (*a*-Ge) films grown by dc magnetron sputtering from pure (99.9999%) Ge targets on glass substrates at room temperature. Their thicknesses were 50, 80, 100 and 130 nm. The room thermal conductivity of the films[14] and the glass substrate[15] are k

[a)]Author to whom correspondence should be addressed; electronic mail: fvega@oo.upc.es
[b)]Present address: Laboratoire de Chimie et Application, Institut Universitaire de Technologie de Metz-Département Chimie-Rue victor Demange 57500 Saint-Avold, France

 © 2003 American Institute of Physics

Downloaded 23 Jan 2013 to 161.111.22.141. Redistribution subject to AIP license or copyright; see http://jap.aip.org/about/rights_and_permissions

$=0.010$ and $k=2.8\times10^{-3}$ W K^{-1} cm^{-1}, respectively. The real and imaginary parts of the refractive indices of the films have been reported elsewhere.[16]

The experimental setup used to irradiate the films and to perform the real time reflectivity (RTR) measurements, has been described extensively elsewhere.[13,17,18] A dye laser amplifier (sulforhodamine 6), pumped with the second harmonic of a *Q*-switched Nd: yttrium–aluminum–garnet laser ($\lambda=532$ nm), was seeded with the output of a continuous wave (cw) dye laser (rhodamine 6 G) tuned at $\lambda=584$ nm, and pumped with an Ar^+ laser operating at $\lambda=514$ nm. The amplified output beam [$\lambda=584$ nm, pulse duration $\tau=6$ ns full width at half maximum (FWHM)] was spatially filtered before being focused at normal incidence onto the sample surface to a spot size of several hundreds of microns. The irradiation of the samples was carried out in air and each time a fresh region of the film was exposed to a single laser pulse.

The structural transformation dynamics was followed in real time by measuring the reflectivity changes induced by the pump pulse by means of a single-mode, low-power, cw argon ion laser ($\lambda=514.5$ nm). This probe beam was *s*-polarized and was focused to a 50-μm-diam spot onto the center of the irradiated area. The incidence angle was $\approx15°$. The specular reflection of this beam at the film surface was simultaneously collected by both a fast photodiode connected to a transient digitizer (time resolution of a few ns over a time window of 200 ns) and an ultrafast detection system based on a single sweep streak camera,[13] the latter providing subnanosecond time resolution (typically 350 ps over a time window of 50 ns).

In order to correlate the time evolution of the reflectivity at the probe wavelength with the characteristics of the melting process, optical simulations of the reflectivity changes expected upon film melting have been carried out for all films. For this purpose, a home-developed computer program based on the theory of the optical reflection of thin multilayer films[19,20] was used. The program takes into account both the incidence angle and polarization of the probe beam and calculates the evolution of the surface reflectivity by transforming the optical constants of the *a*-Ge films into the constants of liquid Ge (*l*-Ge). The calculations are done modifying the film structure layer by layer as a liquid–solid interface propagates in depth.

III. RESULTS

Since the *a*-Ge films have different thicknesses, they have different initial reflectivity. To ease the comparison of the results, the reflectivity changes for each film thickness have thus been normalized to the initial reflectivity value of the film/glass-substrate system. Figure 1 shows representative real time reflectivity transients obtained upon irradiation of the 100-nm-thick film at low [Fig. 1(a)] and high fluences [Fig. 1(b)]. Transients recorded using a streak camera (subnanosecond resolution) and a fast photodiode connected to a transient digitizer (nanosecond resolution) have both been included in order to clearly show the influence of the time resolution in the evolution of the reflectivity.

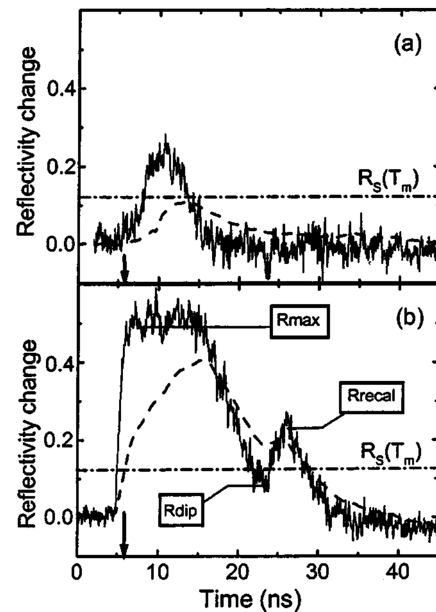

FIG. 1. Real time reflectivity (RTR) transients recorded upon ns laser pulse irradiation of a 100 nm *a*-Ge film on glass at (a) 77 mJ/cm^2 and (b) 220 mJ/cm^2. RTR transients recorded with ns resolution (dashed curve) and subnanosecond resolution (solid curve) are included. The horizontal dash-dotted line indicates the reflectivity level $Rs(Tm)$ expected for the film at its melting temperature. The arrows indicate the temporal location of the maximum of the irradiation pulse (6 ns FWHM).

For low fluences and for the transient recorded with subnanosecond time resolution [Fig. 1(a) solid line], the pump pulse induces a smooth reflectivity increase up to a maximum value above the reflectivity of the solid material at the melting temperature [$Rs(T_m)$],[21] the latter indicating that surface melting has occurred. After the maximum, the reflectivity decreases as a consequence of the solidification of the melted layer once the laser pulse has ended. At higher fluences, the subnanosecond resolution transient [Fig. 1(b) solid line] shows an abrupt increase of the reflectivity up to a plateau, the latter being related to the formation of an optically thick liquid layer. This plateau is followed by a decrease to a minimum (dip), to increase again up to values well above $Rs(T_m)$. Similar oscillations in the solidification tail of the transients have earlier been reported upon irradiation with picosecond laser pulses and identified as the effect of recalescence, i.e., a reheating process due to the massive release of the solidification enthalpy as a consequence of bulk solidification.[7,13,22] The values of the reflectivity at the first (R_{max}) and second (R_{recal}) maxima and at the dip (R_{dip}), are indicated in Fig. 1(b) and will be used to describe the dependence of the melting and solidification processes on the laser fluence and the film thickness.

The effect of the time resolution on monitoring both the melting and the solidification processes can clearly be seen in Fig. 1 by comparing the transients obtained with subnanosecond resolution (solid lines) to those obtained with nanosecond resolution (dashed lines). A poorer time resolution leads to an apparent slower reflectivity increase upon film heating and melting independently of the fluence used. As a consequence, the temporal position of the first reflectivity maximum is shifted to longer time values. Moreover, the

Downloaded 23 Jan 2013 to 161.111.22.141. Redistribution subject to AIP license or copyright; see http://jap.aip.org/about/rights_and_permissions

maximum values of the reflectivity measured with ns resolution are always lower than those ($R_{\max}$) obtained with sub-ns resolution. Thus, the determination of the melting threshold from the RTR transients recorded with ns resolution would lead to an overestimated value. This is clearly shown in Fig. 1(a) where the value of $R_{\max}$ is clearly above $Rs(T_m)$ (i.e., the film is already melted), while in the simultaneously recorded transient with ns resolution the reflectivity maximum is below that value, which would be misinterpreted as simple surface heating.

For higher fluences [Fig. 1(b)], the most outstanding feature of the transients obtained with subnanosecond resolution in comparison with those obtained with nanosecond resolution is the existence of a reflectivity dip with a value around or below $Rs(T_m)$. The decay of the reflectivity from the plateau to the dip has been related to the nucleation of the solid phase throughout the molten volume. The release of the corresponding solidification enthalpy reheats the material.[9–12] In the case of the measurements performed with ns resolution, this recalescence effect is seen as a *shoulder* that appears in the cooling tail of the RTR transients. Thus, the process has very often been described[9–11] in terms of a slowdown of the solidification process as a consequence of the increase of the liquid temperature. The shoulder becomes a clear dip followed by a well-resolved second maximum when the time resolution is sufficiently increased.

The final reflectivity value of the irradiated films, achieved once the whole process of melting, solidification, and cooling has been completed (R_{fin} hereafter), can be used to identify the phases finally formed. Since the whole process lasts typically hundreds of ns that is beyond the longest time window available for the streak camera, R_{fin} has been determined by using a photodiode connected to the transient digitizer. Given the time scale involved, these measurements are not affected by the lower time resolution of this latter system. Since R_{fin} is typically measured 150 ns after the laser pulse, it could be argued that R_{fin} would correspond to a slightly hot material rather than to the reflectivity of the material at room temperature. We have checked this is not the case by recording the room temperature reflectivity several seconds after the pump laser was switched off. In all cases we have found the same value ($\pm 2\%$) than R_{fin}.

The dependence of the characteristic parameters ($R_{\max}$, R_{dip}, R_{recal}, and R_{fin}) on fluence was similar no matter the film thickness. Two representative cases (80 and 100 nm films) have been plotted in Fig. 2. The melting threshold, defined as the fluence for which $R_{\max}$ overcomes $Rs(T_m)$,[21] can be easily identified in the plots. By comparing Figs. 2(a) and 2(c) it can be concluded that the melting threshold of the 100-nm-thick film is higher than that of the 80-nm-thick film.

The fluence threshold for recalescence is defined as the minimum fluence for which the second maximum (R_{recal}) is observed in the transients. This threshold has been indicated in Figs. 2(b) and 2(d) by vertical dotted lines. It is clearly seen that the final reflectivity value of the films (R_{fin}) starts to decrease below the initial value for fluences above the recalescence threshold. Thus, there is a strong correlation between the occurrence of recalescence and the formation

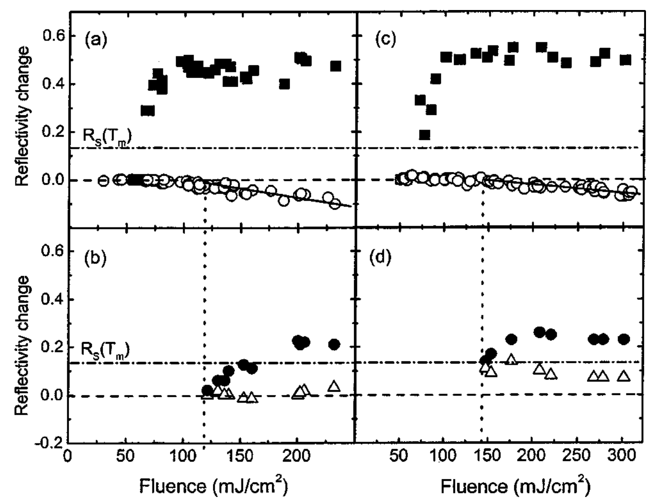

FIG. 2. (a) Maximum transient reflectivity (■) ($R_{\max}$) and final reflectivity (○) (R_{fin}), and (b) reflectivity values at the second maximum (●) (R_{recal}) and at the dip between maxima (△) (R_{dip}), as a function of the laser fluence in the 80 nm *a*-Ge film. (c) and (d) Same as before but in the 100 nm film. The horizontal dash-dotted line indicates the reflectivity level $Rs(Tm)$ expected for the film at its melting temperature.

upon solidification of a material with optical properties different than the initial ones. It can also be noticed that the recalescence threshold is film thickness dependent.

The reflectivity values at the dip (R_{dip}) do not show any significant dependence on fluence [see Figs. 2(b) and 2(d)] and are always below or in the order of $Rs(T_m)$ depending on the film thickness. The reflectivity values corresponding to the second maximum (R_{recal}) increase slightly as the fluence is increased [see Figs. 2(b) and 2(d)]. In the case of the 80-nm-thick film [Fig. 2(b)], the values of R_{recal} are below $Rs(T_m)$ in the neighborhood of the threshold which is an indication that the film initially solidified is only reheated by the release of the solidification enthalpy. Once the fluence is further increased, remelting of the film occurs. In the case of the 100-nm-thick film [Fig. 2(d)], the values of R_{recal} are always above $Rs(T_m)$ that indicates that the solidification enthalpy partially remelts the film.

The thresholds for melting and recalescence are plotted in Fig. 3 as a function of the film thickness.[23] At first glance, both thresholds tend to increase as the film thickness is increased. An exception to this general behavior is the recales-

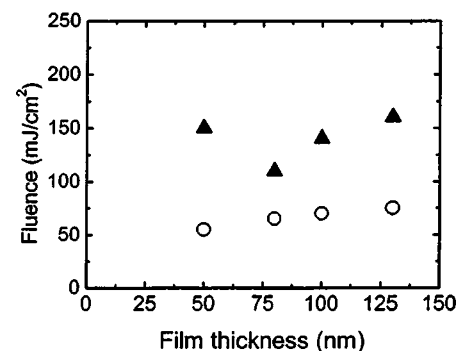

FIG. 3. Melting threshold (○) and recalescence threshold (▲) as a function of the Ge film thickness.

Downloaded 23 Jan 2013 to 161.111.22.141. Redistribution subject to AIP license or copyright; see http://jap.aip.org/about/rights_and_permissions

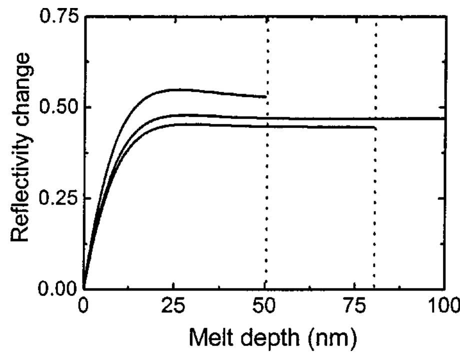

FIG. 4. Simulation of the reflectivity change at the probe wavelength ($\lambda = 514$ nm) expected as a liquid Ge layer progresses in depth in 50, 80, and 100 nm *a*-Ge films on glass.

cence threshold of the 50-nm-thick film (the thinnest film studied) that exhibits a value higher than that of the 80-nm-thick film.

Figure 4 shows the calculated reflectivity changes upon film melting as a function of the melt depth. The refractive indices (n-$i\kappa$) at the probe wavelength (514 nm) used for the calculations were $n_{a\text{-Ge}}=4.73$ $\kappa_{a\text{-Ge}}=2.21$, $n_{l\text{-Ge}}=2.51$ $\kappa_{l\text{-Ge}}=5.12$, and $n_{\text{glass}}=1.52$ (see Refs. 16, 24 and 25, respectively). Results for the 50-, 80-, and 100-nm-thick films are included in the figure. The behavior of the 130-nm-thick film is similar to that of the 100-nm-thick film and is not included. The comparison of these curves to the experimentally determined evolution of the reflectivity $R_{\max}$ [Figs. 2(a) and 2(c)], allows the determination of the melt depth for a given film thickness, provided that the melt depth is sufficiently shallow (typically below 15 nm). Larger melt depths behave optically as opaque layers and the probe beam becomes insensitive to any further increase of the melt depth. The corresponding melt depths as a function of the laser fluence are shown in Fig. 5. The melt depths induced in the 80-, 100-, and 130-nm-thick films follow a nearly linear dependence with the fluence. Moreover, for a given fluence, the melt depth decreases with increasing film thickness. Again, the 50-nm-thick film exhibits a clearly distinct behavior since its melt depth is always smaller than that of the 80-nm-thick film at the same fluence.

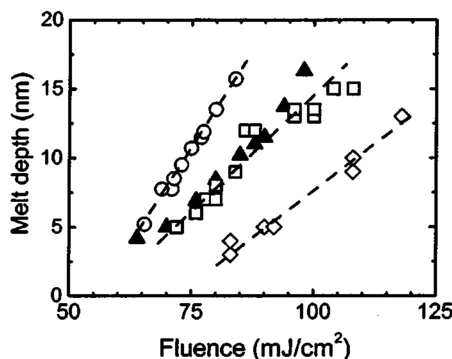

FIG. 5. Calculated melt depth as a function of laser fluence in 50-nm-(▲), 80-nm-(○), 100-nm-(□), and 130-nm-(◇)-thick *a*-Ge films. Lines are included to guide the eye.

IV. DISCUSSION

The analysis of the structural transformation dynamics of *a*-Ge films upon irradiation with nanosecond laser pulses shows that the material behavior is essentially similar to that observed under ps laser pulses.[7] In both cases at high fluences, the appearance of bulk solidification followed by recalescence is evidenced in the reflectivity transients by a dip followed by a well-resolved second maximum. Our results show that the reflectivity values at the dip (R_{dip}) are essentially fluence independent [see Figs. 2(b) and 2(d)] although they exhibit some dependence on the film thickness. For instance, while the 80-nm-thick film shows R_{dip} values close to the initial film reflectivity, the R_{dip} values for the 100-nm-thick film are closer to $Rs(Tm)$. However, regardless the film thickness, R_{dip} is in all cases similar or lower than the reflectivity of the amorphous material at the melting temperature [$Rs(Tm)$] indicating that the material solidifies in the first stage of the process. As a consequence of the release of the solidification enthalpy, the material is reheated (recalescence effect) giving rise to the appearance of a well resolved second reflectivity maximum. It can thus be concluded that the recalescence process manifests itself as a delayed effect after the initial and complete solidification of the film and not, as discussed by several authors before, as a slowdown of the solidification process in a highly undercooled liquid.[9,10,26] This new feature of the solidification dynamics has obviously been possible to observe due to the improved time resolution of the experiment, which allows us to separate neatly the end of the early bulk solidification stage and the reheating effect caused by recalescence. The reflectivity transients show that the recalescence manifests either as "simple" reheating of the surface material [$R_{\text{recal}} \leqslant Rs(Tm)$] or as a remelting process [$R_{\text{recal}} > Rs(Tm)$]. Thus, it can be concluded that remelting induced by recalescence always occurs *after* complete solidification of thin *a*-Ge films melted with either ps[7] or ns laser pulses.

The results show that a fluence threshold (Fig. 3) and thus a minimum melt depth is required for recalescence to be observed. The minimum melt depth required is related to the need for inducing a sufficiently long lasting melt process. Under these conditions and due to both the low thermal conductivity of the glass substrate and the high thermal conductivity of liquid Ge, the heat becomes essentially confined in the film with a negligible temperature gradient throughout the melted layer, so that a bulk solidification process is promoted.[11] Additionally, such a minimum melt depth is also necessary to release a sufficient amount of heat upon bulk solidification to make the recalescence effect observable.[11,27] In particular, it was shown in Ref. 11 that it is possible to substantially reduce the effects of recalescence by simply decreasing the film thickness and thus the total amount of solidification enthalpy released.

Figure 2 shows that at high pulse fluences (at which recalescence always occurs) the final reflectivity of the films (R_{fin}) is lower than the initial one. Actually, there is an excellent agreement between the recalescence threshold and the onset of the decrease of R_{fin}. This decrease indicates the presence of the crystalline phase upon solidification and

Downloaded 23 Jan 2013 to 161.111.22.141. Redistribution subject to AIP license or copyright; see http://jap.aip.org/about/rights_and_permissions

cooling of the films[12,28] as has been previously shown from Raman spectroscopy measurements in films irradiated with ns and ps laser pulses. In those films, the observation of final reflectivity values similar to the one observed in our case was correlated to the formation of a mixture of amorphous and crystalline phases with crystalline fraction increasing with the laser fluence.[7,17,29] It can thus be concluded that the presence of strong recalescence effects after bulk solidification leads to clear changes in the structure of the final material.

Some other aspects of the melting and rapid melting-solidification dynamics of the Ge films on glass under ns pulses deserve further comment. Regarding the evolution of the melting threshold as a function of the film thickness, Fig. 4 shows a slightly increasing tendency versus film thickness, in contrast to the earlier reported decreasing behavior of thresholds for *a*-Ge films grown on Si.[14] This latter substrate has a thermal conductivity[30] (at room temperature) of 1.4 $\mathrm{W\,cm^{-1}\,K^{-1}}$, which is about three orders of magnitude larger than that of the glass substrate used in this work ($2.8\times10^{-3}\ \mathrm{W\,cm^{-1}\,K^{-1}}$). In our case, the "effective" thermal conductivity of the *a*-Ge film/glass-substrate system would range from the value of a bare glass substrate for very thin films, to that of "bulk" *a*-Ge ($0.01\ \mathrm{W\,cm^{-1}\,K^{-1}}$) for the thicker films. As a consequence, the thicker films show a higher effective thermal conductivity that reduces the temperature rise induced upon irradiation at a given fluence.[31] A higher fluence is thus required to reach the melting temperature as the effective thermal conductivity of the film/substrate-system increases, in agreement with what is experimentally observed in this work. In the case of *a*-Ge films on Si, the evolution of surface temperature is just the opposite, since the thicker the film the lower the effective thermal conductivity of the film-Si substrate system.[14]

The same explanation holds for the dependence of the melt depth on the laser fluence in the 80-, 100-, and 130-nm-thick films shown in Fig. 5: the thicker the film, the lower the surface temperature and thus the lower the melt depth. Following this reasoning, one would expect melt depth values in the 50-nm-thick film larger than those obtained in the 80-nm-thick film. However, there is another parameter influencing the surface temperature that is the laser fluence really *absorbed* in the film. The imaginary part of the refractive index[16] at the irradiation wavelength ($\lambda=584$ nm) of the *a*-Ge is $\kappa=1.77$ which leads to a skin penetration depth of $\approx$26 nm.[32] The amount of intensity that reaches the transparent glass substrate after passing through the film can be calculated by using the Beer–Lambert law for the linear absorption of the laser intensity.[33] In the case of the 50-nm-thick film, it is estimated that a fraction of 14% of the laser intensity reaches the film/substrate interface and nearly all of it is transmitted through the transparent substrate. The intensity fraction arriving at the substrate decreases to 5% in the case of the 80-nm-thick film and is below 3% in the case of the 100 nm and 130-nm-thick films. The distinct behavior observed in the 50-nm-thick film is then most likely related to the fact that the lower effective thermal conductivity of this film/substrate system is compensated by the fact that a high fraction of the beam intensity is directly coupled *into* the glass substrate and then transmitted. The same effect could also explain the high value of the recalescence threshold found in the 50-nm-thick film (see Fig. 3). Since this threshold is related to a minimum melt depth, the result shown in Fig. 3 agrees with the lower laser fluence absorbed in the 50-nm-thick film and the consequently smaller melt depths induced.

V. CONCLUSIONS

The sequence of events occurring during melting and rapid solidification of *a*-Ge films on glass melted with ns laser pulses has neatly been identified by means of real time reflectivity measurements with subnanosecond resolution. Bulk solidification followed by remelting occurs once a minimum melt depth is induced upon irradiation. This minimum melt depth that is film thickness dependent, is related on one hand, to the need for a sufficiently long lasting melting process required to suppress the thermal gradient across the molten layer and, on the other hand, to the release of a sufficient amount of heat upon bulk solidification. In all cases, the film solidifies completely in the initial stage of the process. At fluences above the recalescence threshold, the massive release of the solidification enthalpy can eventually induce partial remelting of the film. The material produced once the whole process has been completed corresponds to a mixture of amorphous and crystalline phases as deduced from its optical properties. Finally, the dependence of the melt depth on fluence for films of different thickness can be explained in terms of two effects with opposite results: the amount of the laser intensity that reaches the substrate without being absorbed in the film and the effective thermal conductivity of the film/substrate system.

ACKNOWLEDGMENTS

This work has been partially supported by the European Union in the framework of the TMR ERB FMRX CT098-0188 "Laser Cleaning" Network. N.C. acknowledges the funding of the European Union through the same contract.

[1] M. Matsumura and Ch. Oh, Thin Solid Films **337**, 123 (1999).
[2] F. J. Adrian, J. Bohandy, B. F. Kim, A. N. Jette, and P. T. Thompson, J. Vac. Sci. Technol. B **5**, 1490 (1987).
[3] M. Hatano, S. Moon, M. Lee, K. Suzuki, and C. Grigoropoulos, J. Appl. Phys. **87**, 36 (2000).
[4] M. Lee, S. Moon, M. Hatano, K. Suzuki, and C. Grigoropoulos, J. Appl. Phys. **88**, 4994 (2000).
[5] L. Brambilla, L. Colombo, V. Rosato, and F. Cleri, Appl. Phys. Lett. **77**, 2337 (2000).
[6] P. V. Santos, A. Trampert, F. Doudeo, D. Comedi, H. J. Zhu, K. H. Ploog, A. R. Zanatta, and I. Chambouleyron, J. Appl. Phys. **90**, 2575 (2001).
[7] J. Siegel, J. Solis, and C. N. Afonso, Appl. Phys. Lett. **75**, 1071 (1999).
[8] J. Siegel, J. Solis, C. N. Afonso, F. Vega, J. Bankmann, O. Martinez-Sacristan, and K. Sokolowski-Tinten, J. Appl. Phys. **89**, 3642 (2001).
[9] S. R. Stiffler, M. O. Thompson, and P. S. Peercy, Phys. Rev. Lett. **60**, 2519 (1988).
[10] S. R. Stiffler, M. O. Thompson, and P. S. Peercy, Appl. Phys. Lett. **56**, 1025 (1990).
[11] T. Sameshima and S. Usui, J. Appl. Phys. **74**, 6592 (1993).
[12] J. Siegel, J. Solis, C. N. Afonso, and C. García, J. Appl. Phys. **80**, 6677 (1996).
[13] J. Solis, J. Siegel, and C. N. Afonso, Rev. Sci. Instrum. **71**, 1595 (2000).
[14] W. Szysko, F. Vega, and C. N. Afonso, Appl. Phys. A: Mater. Sci. Process. **61**, 141 (1995).

Downloaded 23 Jan 2013 to 161.111.22.141. Redistribution subject to AIP license or copyright; see http://jap.aip.org/about/rights_and_permissions

[15] J. Solis and C. N. Afonso, J. Appl. Phys. **72**, 2125 (1992).
[16] J. C. G. de Sande, C. N. Afonso, J. L. Escudero, R. Serna, F. Catalina, and E. Bernabeu, Appl. Opt. **31**, 6133 (1992).
[17] J. Siegel, J. Solis, and C. N. Afonso, J. Appl. Phys. **84**, 5531 (1998).
[18] N. Chaoui, J. Siegel, J. Solis, and C. N. Afonso, J. Appl. Phys. **89**, 3763 (2001).
[19] H. A. Macleod, *Thin Film Optical Filters*, 2nd ed. (Hilger, London, 1986).
[20] F. Vega, J. Solis, J. Siegel, and C. N. Afonso, J. Appl. Phys. **88**, 6321 (2000).
[21] The reflectivity changes are measured as deviations from the initial reflectivity of the film. As a consequence, the reflectivity of the solid material at the melting temperature $Rs(Tm)$ depends on the film thickness, being about 10%–14% above the initial reflectivity of the film (see Refs. 15 and 17). A "reference" value of $Rs(Tm)=12\%$ has been included in the figures.
[22] J. Solis, J. Siegel, and C. N. Afonso, Appl. Surf. Sci. **154–155**, 499 (2000).
[23] To ease the comparison to earlier results, the melting threshold of a 50-nm-thick *a*-Ge film on glass upon picosecond pulses was 15 mJ/cm^2 (see Ref. 7).
[24] G. E. Jellison and D. H. Lowndes, Appl. Phys. Lett. **51**, 352 (1987).
[25] E. D. Palik, *Handbook of Optical Constants of Solids* (Academic, New York, 1985).
[26] S. R. Stiffler, M. O. Thompson, and P. S. Peercy, Phys. Rev. B **43**, 9851 (1991).
[27] F. Vega, C. N. Afonso, W. Szyszko, and J. Solis, J. Appl. Phys. **82**, 2247 (1997).
[28] F. Vega, R. Serna, C. N. Afonso, D. Bermejo, and G. Tejeda, J. Appl. Phys. **75**, 7287 (1994).
[29] J. Solis, J. Siegel, C. Garcia, J. Jimenez, and R. Serna, Mater. Res. Soc. Symp. Proc. **452**, 839 (1997).
[30] S. de Unamuno and E. Fogarassy, Appl. Surf. Sci. **36**, 1 (1989).
[31] M. von Allmen and A. Blatter, *Laser-Beam Interactions with Materials*, 2nd ed., Springer Series in Materials Science (Springer, Berlin, 1987), Chap. 3, pp. 44–47.
[32] The linear absorption coefficient is defined as $\alpha=4\pi\kappa/\lambda$
[33] According to the Beer–Lambert law, the laser intensity at any film depth z is $I=(1-R)I_o\exp(-\alpha z)$, R being the film reflectivity and I_o the laser intensity that strikes the sample surface.

Downloaded 23 Jan 2013 to 161.111.22.141. Redistribution subject to AIP license or copyright; see http://jap.aip.org/about/rights_and_permissions